24th COBEM - 2017

24th ABCM International Congress of Mechanical Engineering
December 3-8, 2017, Curitiba, PR, Brazil

COBEM-2017-1266
BOUNDARY LAYER ANALYSIS OF TURBULENCE-RADIATION INTERACTION IN A NON-REACTIVE CHANNEL FLOW

Guilherme Crivelli Fraga
Adriane Prisco Petry
Francis Henrique Ramos França
Universidade Federal do Rio Grande do Sul, Department of Mechanical Engineering, Av. Paulo Gama, 110, Porto Alegre, RS, Brazil
guilhermecfraga@ufrgs.br
adrianep@mecanica.ufrgs.br
frfranca@mecanica.ufrgs.br

Abstract. *This paper presents a continuation of an analysis on turbulence-radiation interaction (TRI) effects in a non-reacting channel flow of a homogeneous participating gas. It is investigated the behavior of the relative difference between the mean volumetric radiative heat source obtained by solutions considering and neglecting TRI effects, which, in a previous study, was observed to have an almost totally smooth three-dimensional field, interrupted by a few points where the local difference rose abruptly to values exceptionally high. To obtain the data for the analysis, simulations are conducted in the open-source code Fire Dynamics Simulator, using Large Eddy Simulation to generate transient fields of the quantities of interest. Results show that the points of maximum of the difference are attributed to the local mean radiative heat source approaching zero in a region of relative coarse spatial discretization. In a second part of the study, seeing that the points of spike in the difference are located near the domain walls, TRI effects inside the thermal boundary layer are investigated, from which it is found that all points of maximum are located inside that layer. When only the region outside of the boundary layer is considered, a totally smooth field of the relative difference is obtained, with domain-averaged values of the difference agreeing with what is expected from the literature.*

Keywords: *Turbulence-radiation interaction, boundary layer, Large Eddy Simulation, Fire Dynamics Simulator*

1. INTRODUCTION

Turbulence-radiation interaction (TRI) is a phenomenon promoted by the highly non-linear coupling between fluctuations of radiation intensity, caused by turbulence, and fluctuations of temperature and medium composition. The importance of TRI has been demonstrated experimentally, theoretically and numerically for a variety of turbulent problems (Coelho, 2007), and its effects manifest as a difference observed between predicted time-averaged quantities and the same quantities computed neglecting turbulent fluctuations (i.e., calculated from mean temperature and species concentration fields).

In previous studies, the authors investigated the magnitude of TRI effects for a series of cases involving a non-reactive channel flow of a high temperature homogeneous gas (Fraga et al., 2015; Fraga et al., 2016; Fraga et al., 2017). The mean volumetric radiative heat source calculated from numerical simulations considering turbulent fluctuations of temperature was compared with the radiative heat source obtained neglecting those fluctuations. This resulted in three-dimensional fields of the relative difference between those quantities, which allowed the authors to assess the importance of turbulence-radiation interaction for the studied cases. From these fields, it was observed that the relative difference had an overall smooth distribution throughout the majority of the calculation domain, and its value was in agreement with other works on TRI in non-reactive problems. However, in some particular points, the difference presented values exceptionally large, dissonant with its surrounding distribution and much above what is expected for the magnitude of TRI effects even for the most critical types of problems. In the studies cited earlier, this behavior was only briefly mentioned and not discussed further. Therefore, the main motivation and objective of the present paper is to investigate the reasons behind this behavior and propose a methodology to avoid such occurrences in future analyses.

In the second part of the study, recognizing that the abrupt increases, or spikes, in the relative difference occurred especially near the domain walls, the turbulence-radiation interaction inside the boundary layer is investigated. This is a relative unexplored subject of research: a few works in the area of meteorological research have studied the influence of thermal radiation inside the (planetary) boundary layer (Prinn, 1977; Coantic and Simonin, 1984; Curry, 1985), and a single study more focused on engineering problems is presented by Duan et al. (2011), in which Direct Numerical Simulation (DNS) was used to evaluate TRI effects on the radiative emission inside the hypersonic turbulent boundary layer

formed around a reentry vehicle at peak heating condition. However, as far as the authors' knowledge, in the framework of internal flows, TRI effects inside the boundary layer have not been studied previously.

2. PROBLEM STATEMENT

Turbulence-radiation interaction is investigated in the context of a non-reactive channel flow of a homogeneous participating gas. The gas is composed either entirely of carbon dioxide or entirely of water vapor; mixtures between these two species or dilution with non-participating species are not considered. Geometry and boundary conditions are similar to the configuration and the parameters adopted by Fraga et al., 2017, and are shown in Fig. 1.

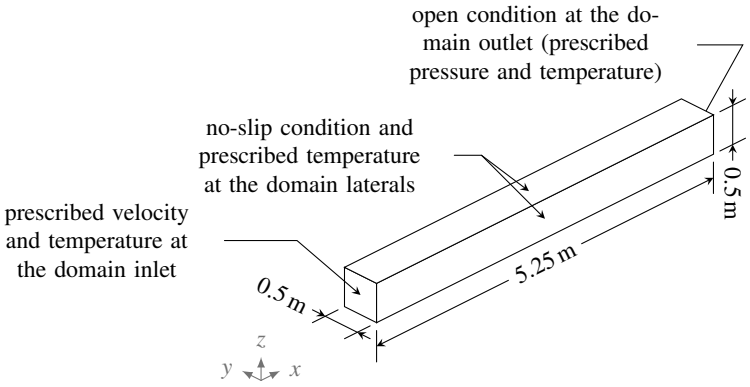

Figure 1: Geometry and boundary conditions of the problem.

The flow develops inside a square duct of lateral dimensions equal to 0.5 m and length equals to 5.25 m. At the front opening of the duct, gas at a spatially uniform and temporally constant temperature of 1200 K is injected with a Reynolds number of 5100. Turbulence fluctuations are imposed at the inlet using the Synthetic Eddy Method (Jarrin, 2008), considering a range of turbulence intensities, IT, between 0 and 20 %. The walls of the duct are kept at a constant and uniform temperature of 400 K and are treated as black surfaces for the radiative heat transfer calculations. On the opposite surface to the inlet, it is assumed an open condition to an outside environment maintained at atmospheric pressure and composed of the same species as the gas flowing inside the duct. The environment is assumed to behave as a blackbody at constant temperature; this temperature is taken as equal to the bulk mean temperature calculated at the cross-sectional plane of grid cells adjacent to the outlet surface. For each studied case, the determination of this temperature requires an iterative procedure, described in details in Fraga et al., 2016 and Fraga et al., 2017.

3. METHODOLOGY

3.1 Transport equations and turbulence modeling

The transport equations for mass, momentum and energy are solved for a three-dimensional, transient, non-isothermal, compressible flow of a single non-reacting species in a Cartesian coordinate system. To simplify the governing equations and facilitate the numerical solution, the low Mach number (Rehm and Baum, 1978) approximation is introduced; this allows the separation of the total pressure in a background component, which is solved by the equation of state (assuming ideal gas behavior), and a pressure fluctuation, for which an additional Poisson equation is introduced (McGrattan et al., 2017a).

Large-eddy simulation (LES) is adopted to capture the transient fluctuations, through the application of a low-pass box filter (of width dependent on the grid cell size) to the transport equations. A constant turbulent Prandtl number equal to 0.5 is used, and, for the closure of the LES transport equations, the dynamic Smagorinsky model (Germano et al., 1991; Lilly, 1992) is employed. Further informations on the transport equations and turbulence modeling can be found in a previous paper by the authors (Fraga et al., 2017).

3.2 Radiation modeling

To determine the thermal radiation field, the radiative heat transfer equation (RTE) is solved. For non-scattering media, as it is assumed for the cases studied here, the RTE is given by (Howell et al., 2010; Modest, 2013):

$$\frac{\mathrm{d}I}{\mathrm{d}s} = \kappa_\eta I_{b\eta} - \kappa_\eta I_\eta \tag{1}$$

where η is the radiation wavenumber; s is the coordinate along the path of radiation; κ_η is the spectral absorption coefficient of the medium; and I_η and $I_{b\eta}$ are the spectral radiation intensity and the blackbody spectral radiation intensity, respectively.

The RTE and the energy transport equation are coupled through the volumetric radiative heat source, S_r, defined as the negative of the radiative heat flux divergence:

$$S_r = -\nabla \cdot \mathbf{q} = \int_0^\infty \kappa_\eta \left(G_\eta - 4\pi I_{b\eta} \right) \, \mathrm{d}\eta \tag{2}$$

in which $\mathbf{q}$ is the radiative heat flux vector and G_η is the spectral incident radiation, given as the integration of the spectral intensity over all solid angles Ω:

$$G_\eta = \int_{4\pi} I_\eta \, \mathrm{d}\Omega \tag{3}$$

For the solution of the radiative heat transfer problem, the spatial and spectral integrations of Eqs. (1) and (2) are required—i.e., an integration over all directions of radiation propagation and an integration over all the radiation spectrum. For the former, the finite volume method (Raithby and Chui, 1990) is used. This method divides the unit sphere surrounding each point in a finite number of solid angles, inside which the radiation intensity is assumed to be constant relative to direction; then, the RTE is solved for each angle and the continuous integral over the unit sphere, Eq. (3), is approximated as a weighted summation over the results for all discrete angles.

The spectral integration is performed using the Weighted-Sum-of-Gray-Gases (WSGG) model. This is a spectral model relatively simple to implement and with low computational cost, which has shown good agreement with line-by-line integration (benchmark solution) results for a number of different situations (Dorigon et al., 2013; Cassol et al., 2014). In the WSGG model, the spectrum of radiation is replaced by N_j gray gases with uniform absorption coefficients and by transparent windows. The RTE for the jth gas may then be written as:

$$\frac{\mathrm{d}I_j}{\mathrm{d}s} = \kappa_j a_j I_b - \kappa_j I_j \tag{4}$$

where I_j and κ_j are the radiative intensity and the absorption coefficient of gas j, respectively. The term a_j is named the temperature coefficient and represents the fraction of blackbody radiation emitted at the local temperature of the medium in the wavenumber interval correspondent to the jth gas. The coefficient a_j is described as a polynomial function of the temperature T,

$$a_j = \sum_{k=0}^{4} b_{j,k} T^k \tag{5}$$

The polynomial coefficients $b_{j,k}$ in this equation, as well as the pressure-absorption coefficient $\kappa_{p,j}$ of each gray gas (defined as the ratio between the absorption coefficient and the partial pressure of the participating species), are obtained from fitting global radiation data (typically, of total emittance). In the present study, the values of those coefficients are taken from the work of Cassol et al. (2014) and are given in Tabs. 1 and 2 for the two participating species considered (carbon dioxide and water vapor, respectively).

Table 1: WSGG model coefficients for a participating gas composed entirely of carbon dioxide (Cassol et al., 2014).

j	$\kappa_{p,j}$ (atm^{-1} m^{-1})	$b_{j,0}$	$b_{j,1}$ (K^{-1})	$b_{j,2}$ (K^{-2})	$b_{j,3}$ (K^{-3})	$b_{j,4}$ (K^{-4})
1	0.138	0.0999	64.41×10^{-5}	-86.94×10^{-8}	41.27×10^{-11}	-67.74×10^{-15}
2	1.895	0.00942	10.36×10^{-5}	2.277×10^{-8}	-2.134×10^{-11}	6.497×10^{-15}
3	13.301	0.14511	-30.73×10^{-5}	37.65×10^{-8}	-18.41×10^{-11}	30.16×10^{-15}
4	340.811	−0.02915	25.23×10^{-5}	-26.10×10^{-8}	9.965×10^{-11}	-13.26×10^{-15}

For the solution of the radiative heat transfer problem, Eq. (4) is solved $N_j + 1$ times ($j = 0$ denotes the transparent windows) and the total radiation intensity is obtained as a summation over the intensities I_j of each gray gas and transparent window. To determine the temperature coefficient for the transparent windows, a_0, the constraint $\sum_{j=0}^{N_j} a_j = 1$, derived from the conservation of energy requirement, is used.

Table 2: WSGG model coefficients for a participating gas composed entirely of water vapor (Cassol et al., 2014).

j	$\kappa_{p,j}$ (atm^{-1} m^{-1})	$b_{j,0}$	$b_{j,1}$ (K^{-1})	$b_{j,2}$ (K^{-2})	$b_{j,3}$ (K^{-3})	$b_{j,4}$ (K^{-4})
1	0.171	0.06617	55.48×10^{-5}	-48.41×10^{-8}	22.27×10^{-11}	-40.17×10^{-15}
2	1.551	0.11045	0.576×10^{-5}	24.00×10^{-8}	-17.01×10^{-11}	30.96×10^{-15}
3	5.562	−0.04915	70.63×10^{-5}	-70.12×10^{-8}	26.07×10^{-11}	-34.94×10^{-15}
4	49.159	0.23675	-18.91×10^{-5}	-0.907×10^{-8}	4.082×10^{-11}	-9.778×10^{-15}

3.3 Numerical procedures

The set of equations described in the previous sections are numerically solved using the open-source Fortran-based computer fluid dynamics code Fire Dynamics Simulator (FDS). The core algorithm of solution consists in an explicit predictor-corrector scheme, with second order accuracy both in time and in space (McGrattan et al., 2017b). The computational domain is discretized in space utilizing staggered, structured, rectilinear meshes. An uniformly-spaced grid with 121 cells in the x-direction and 36 cells in the other directions is adopted, along with a constant time-step of 1×10^{-3} s and 100 finite angles for the solution of the RTE. These choices follow grid, time-step and angular discretization sensibility analyses presented in Fraga et al. (2017).

3.4 Approach to TRI effects evaluation

To evaluate the magnitude of turbulence-radiation interaction effects, results for the mean volumetric radiative heat source field $\overline{S_r}$ calculated from two different solutions are compared. In the first solution, the transient problem is solved using LES for a total time of 20 s and the instantaneous radiative heat source in each point of the domain is averaged over the last 15 s of simulation (analyses performed in longer lasting cases indicated that this time interval is sufficient to provide representative averages). In the remaining of this paper, this approach is denominated the "with TRI" solution. A second solution for $\overline{S_r}$ is obtained form an independent one time-step calculation initialized with mean temperature and flow fields computed from the transient "with TRI" solution; this produces a mean radiative heat source field where turbulent fluctuations are fully neglected, and is named here the "without TRI" solution.

The comparison between "with TRI" and "without TRI" solutions is quantitatively investigated by defining a relative difference ψ, given as:

$$\psi = \left| \frac{\overline{S_r}^{\mathrm{TRI}} - \overline{S_r}^{\mathrm{nTRI}}}{\overline{S_r}^{\mathrm{nTRI}}} \right| \tag{6}$$

where $\overline{S_r}^{\mathrm{TRI}}$ and $\overline{S_r}^{\mathrm{nTRI}}$ are the mean radiative heat source obtained by the "with TRI" and "without TRI" solutions, respectively.

4. RESULTS

The results of this study are divided in three parts. In the first, it is provided a brief description of the apparently anomalous behavior of the relative difference ψ inside the computational domain, observed for the cases simulated in this study. The second part focuses on the determination of the thickness of the thermal boundary layer. Based on this, the final part of this chapter presents an analysis on the magnitude turbulence-radiation interaction effects outside of the thermal boundary layer and the results are compared to those originally obtained.

It should be mentioned that this paper will not present an in-depth analysis on the deviations between "with TRI" and "without TRI" solutions and on how the turbulence-radiation interaction effects correlate with the different parameters of the simulated cases. For this, the reader is referred to previous works by the authors (Fraga et al., 2016; Fraga et al., 2017).

4.1 Investigation on the behavior of the relative difference between "with TRI" and "without TRI" solutions

Since the radiative heat source is a three-dimensional field, ψ can be individually calculated via Eq. (6) for each point inside the domain, resulting in a three-dimensional spatial distribution of the relative difference between the "with TRI" and "without TRI" solutions. Based on this field, a number of statistical quantities may be determined, such as the maximum local ψ and its domain-averaged value, which can then be used to estimate the magnitude of TRI effects. This was done by the authors in previous papers (Fraga et al., 2016; Fraga et al., 2017), with results that, in general, agreed with what is expected from the literature.

However, when a two-dimensional slice of the three-dimensional field of ψ is plotted, a small number of discontinuities

in the behavior of the relative difference is identified. For the majority of the domain, ψ has an overall smooth spatial distribution and its value is relatively small, in agreement with findings of other works on turbulence-radiation interaction in non-reactive flows. In some particular regions of the domain, however, the relative difference rises to values as large as 3×10^6 %, which is much higher than what is predicted for the impact of TRI effects even in the most critical cases. Examples of such occurrence are depicted in Fig. 2, that shows distributions of ψ for two cases simulated with carbon dioxide as the participating medium (for turbulence intensities of incoming flow equal to 5 % and 10 %). From the figure, it is clear that the increase in the relative difference is abrupt and restricted to a very small location inside the domain. It should also be noted that these spikes in the values of ψ are present in all cases simulated in the study and are distributed almost arbitrarily throughout the domain (though the spikes are, in fact, restricted to regions close to the domain walls, as it will be discussed later).

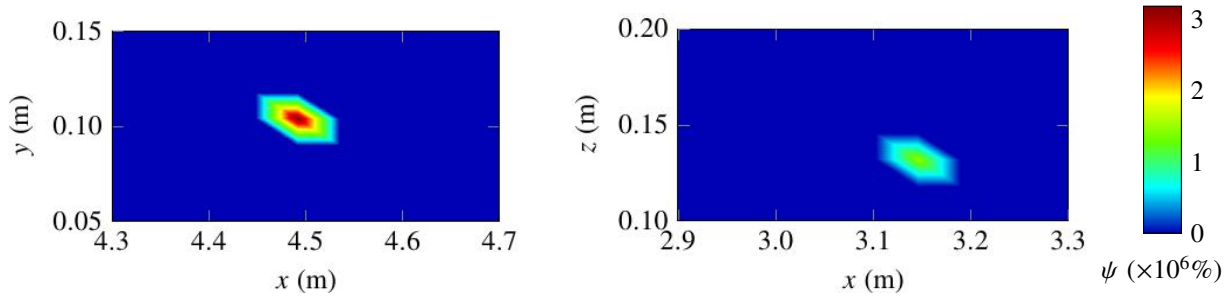

Figure 2: Profile of the local relative difference ψ in regions of spikes, for a medium composed of carbon dioxide with turbulence intensities of the flow at the inlet of 5 % (a) and 10 % (b).

Although only a small number of spikes in ψ are observed, due to the large values of the relative difference in these points there is, as a consequence, an increase in the overall or domain-average difference computed for each case. This is illustrated in Tab. 3, where the maximum local value and the domain-averaged value of ψ are presented for the cases simulated in this paper (under the columns denominated ''ψ – full domain"). As already mentioned, the maximum local difference may be as high as 3×10^6 %, while the domain-averaged difference ranges from 6 % to 27 %; for a non-reactive problem, these magnitude of TRI effects are much greater than what is reported by other similar studies (Mazumder and Modest, 1999; Gupta et al., 2009; Santos et al., 2014).

Table 3: Relative (ψ) and normalized (γ) differences between the mean radiative heat source computed including and neglecting turbulence-radiation interaction, obtained considering the entire domain or only the core region of the flow.

		ψ – full domain (%)		γ – full domain (%)		ψ – core flow (%)	
Medium	IT (%)	Maximum	Average	Maximum	Average	Maximum	Average
CO_2	0	2.934×10^4	6.505	20.461	0.978	0.989	0.117
	5	3.184×10^6	27.622	20.366	1.243	1.088	0.161
	10	1.473×10^6	17.576	21.426	1.564	1.008	0.239
	15	2.859×10^4	5.652	36.808	1.885	1.203	0.319
	20	2.247×10^5	5.651	41.388	2.169	1.230	0.396
H_2O	5	5.716×10^4	6.289	7.305	0.708	0.527	0.134
	10	4.291×10^4	6.544	8.803	0.824	0.466	0.153
	15	7.759×10^5	15.058	13.218	0.943	0.514	0.186
	20	1.412×10^6	25.194	16.121	1.049	0.489	0.201

To better understand the behavior of the local relative difference, Fig. 3 shows ψ and the mean radiative heat flux computed considering and neglecting TRI (i.e., $\overline{S_r}$ obtained by the "with TRI" and "without TRI" solutions, respectively) along lines in the longitudinal direction of the domain that pass through the spike points of ψ depicted in Fig. 2. It is possible to identify low-amplitude oscillations of both $\overline{S_r}^{\mathrm{TRI}}$ and $\overline{S_r}^{\mathrm{nTRI}}$ superposing a well-defined spatial distribution, which agrees with the overall profile of the relative difference between these quantities. The sudden spikes in ψ (located approximately at $x = 4.5$ m in Fig. 3a and at $x = 3.15$ m in Fig. 3b) correspond to regions where the value of $\overline{S_r}^{\mathrm{nTRI}}$ nears zero. This was observed in all cases simulated in the present work and could offer a reason behind the spikes observed

in the ψ fields: if, in positions where $\overline{S_r}^{\mathrm{nTRI}}$ is almost zero, $\overline{S_r}^{\mathrm{TRI}}$ does not have a very similar value, it is expected an increase in the relative difference between these quantities, due to the presence of $\overline{S_r}^{\mathrm{nTRI}}$ in the denominator of Eq. (6).

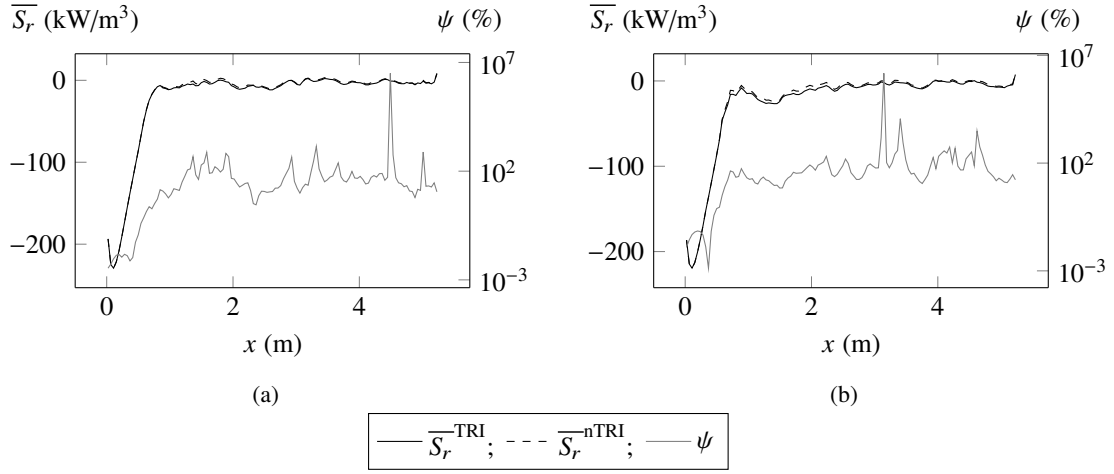

Figure 3: Profiles of the relative difference and the mean radiative heat source computed considering and neglecting turbulence-radiation interaction along lines that passes through the spike points of ψ shown in Fig. 2. The participating medium is carbon dioxide and the turbulence intensity of the flow at the inlet is 5 % (a) and 10 % (b).

However, if this was the complete explanation, the curves for the mean radiative heat source computed by the "without TRI" solution along the x-direction in Figs. 3a and 3b should only approach zero in the small region corresponding to the spikes in ψ, which is not what is verified in those figures. In fact, the figures illustrate that, while $\overline{S_r}^{\mathrm{nTRI}}$ is close to zero for a large region of space, spikes of ψ seem to occur in apparently arbitrary positions inside this region.

A closer inspection on the discrete values of the mean radiative heat source is provided by Figs. 4a and 4b, which present the same curves depicted in Figs. 3a and 3b, but on a narrower region, near the points of spikes of ψ. A gray horizontal line marks the value $\overline{S_r} = 0$, and the "x"es denoting the exact locations inside the domain where the radiative heat source (and, as a consequence, the relative difference) is computed by the numerical grid.

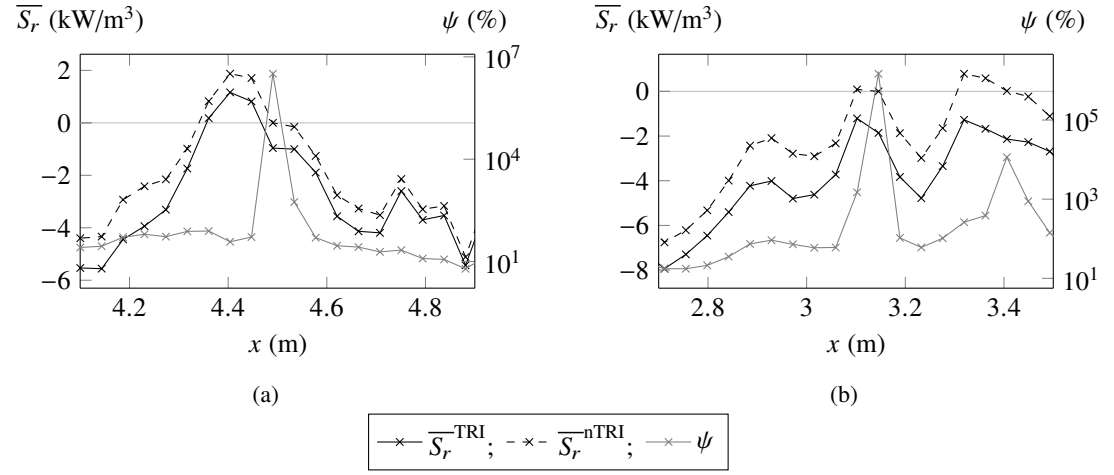

Figure 4: Detailed view of the profiles shown in Fig. 3, with "x"es denoting the locations where the quantities are evaluated by the numerical grid and the gray horizontal line marking the value $\overline{S_r} = 0$. The participating medium is carbon dioxide and the turbulence intensity of the flow at the inlet is 5 % (a) and 10 % (b).

From Fig. 4, it is more clearly noticeable that elevated values of ψ occur at points where the mean radiative heat source computed neglecting turbulent fluctuations approaches zero, with no visual indication that the absolute difference between $\overline{S_r}^{\mathrm{TRI}}$ and $\overline{S_r}^{\mathrm{nTRI}}$ is significantly greater at these locations than at the immediately neighboring points. On the other hand, Figs. 4a and 4b dismiss the idea that the observed behavior of ψ is an anomaly, which could potentially indicate an error in the methodology adopted or in the numerical code used. Instead, the spikes in ψ seems to be a consequence of an increase of $\overline{S_r}^{\mathrm{nTRI}}$ from a negative to a positive value in a small region of the domain (or, conversely, a decrease in the quantity

from a positive to a negative) allied with a poor local spatial discretization. For example, consider a case where the mean radiative heat flux along a given direction rapidly increases from a negative value to a positive one; then, if the numerical grid is not sufficiently fine, a situation may arise in which three neighboring grid points along that direction present values of $\overline{S_r}^{\mathrm{nTRI}}$ that are very negative, very close to zero and very positive, respectively. In this case, if the value of $\overline{S_r}^{\mathrm{TRI}}$ at the center point is slightly different than $\overline{S_r}^{\mathrm{nTRI}}$, the resulting relative difference will be much higher at this point than at the neighboring points.

It should be noted that, if this explanation is correct, then a refinement of the spatial discretization will not eliminate the elevated values of ψ obtained in the simulations of this study, but only increase the number of grid cells for which the relative difference has values exceptionally large (i.e., the number of cells inside the regions of spike in ψ). One solution to eliminate the sporadic maximums of ψ discussed in this section would be to redefine the expression for the difference between $\overline{S_r}^{\mathrm{TRI}}$ and $\overline{S_r}^{\mathrm{nTRI}}$, such as adopting a normalized difference γ, given as

$$\gamma = \left| \frac{\overline{S_r}^{\mathrm{TRI}} - \overline{S_r}^{\mathrm{nTRI}}}{\overline{S_{r\,\mathrm{avg}}}^{\mathrm{TRI}}} \right| \tag{7}$$

where $\overline{S_{r\,\mathrm{avg}}}^{\mathrm{TRI}}$ is the domain-averaged mean radiative heat source obtained from the "with TRI" solution. An approach like this has been adopted by the authors in previous works (Fraga et al., 2017), and, for reference, the maximum and domain-averaged values of γ for all simulated cases are presented in Tab. 3. An alternative methodology to address the occurrence of spikes of ψ, which maintains the relative difference definition, is proposed in the final section of this chapter. Before this, however, a discussion on the identification of the thermal boundary layer thickness for the problem under consideration is necessary.

4.2 Determination of the thermal boundary layer thickness

The thickness δ of the thermal boundary layer is defined as the distance normal to the solid surface at which the local temperature T equals a given fraction of the temperature of the free-stream, T_∞. Although a fraction equals to $0.99T_\infty$ is commonly used to determine the boundary layer thickness (Bergman et al., 2011), in this paper a slightly more conservative value of $0.995T_\infty$ is adopted.

As an illustration, Fig. 5 depicts the results for the boundary layer thickness for simulations with carbon dioxide and water vapor in which the turbulence intensity of the incoming flow is 10 %. In Figs. 5a and 5b, the outline of the thermal boundary layer throughout the three-dimensional domain is presented for cases employing CO_2 and H_2O as the participating gas, respectively, while the curves in Figs. 5c and 5d present a two-dimension visualization of the boundary layer thickness along the central xz plane of the domain for these same cases. Similar profiles were observed for the other simulations and are not shown here for brevity purposes.

Figure 5 indicates that the flow does not reach a thermally developed condition for the entire length of the domain, since a merging of the thermal boundary layers corresponding to the upper and lower surfaces does not occur. For a turbulent flow, the length of the thermal entrance region is expected to be approximately equal to ten times the hydraulic diameter of the channel (Bergman et al., 2011). Therefore, seeing that the domain considered in the present work has a length of 10.5 times its hydraulic diameter, it is possible that, at the domain outlet, the flow is not yet (but about to be) thermally developed.

4.3 Relative difference between "with TRI" and "without TRI" solutions outside the thermal boundary layer

Once the thermal boundary layer thickness is determined for each simulation, all data (in this case, only the mean radiative heat source computed by the "with TRI" or the "without TRI" solutions) corresponding to the inside of the boundary layer is removed and the relative difference between $\overline{S_r}^{\mathrm{TRI}}$ and $\overline{S_r}^{\mathrm{nTRI}}$ is recalculated via Eq. (6). The resulting field of ψ for each simulation is still a three-dimensional distribution, but it includes only points located in the core region of the flow. Based on these fields, new local maximum and domain-averaged values of ψ may be computed, which are shown in Tab. 3 (under the columns denominated "ψ – core flow").

Table 3 evidences that, when neglecting the regions inside the thermal boundary layer, there is a considerable reduction in the relative difference compared to the difference calculated from data of the entire computational domain. The local maximums of ψ inside the core region of the flow are smaller than 1.3 % for all simulated cases, indicating that the sporadic spikes of ψ do not occur inside the core region of the flow. As for the domain-averaged relative difference, reductions of one to two orders of magnitude are verified compared to the results of ψ for the full domain. Values of the maximum and domain-average relative difference in the core region of the flow are comparable to the normalized difference γ computed considering the full domain (also shown in Tab. 3), and their magnitude is similar to what is reported in previous works for the effects of turbulence-radiation interaction in non-reactive problems (Mazumder and Modest, 1999; Gupta et al., 2009; Santos et al., 2014).

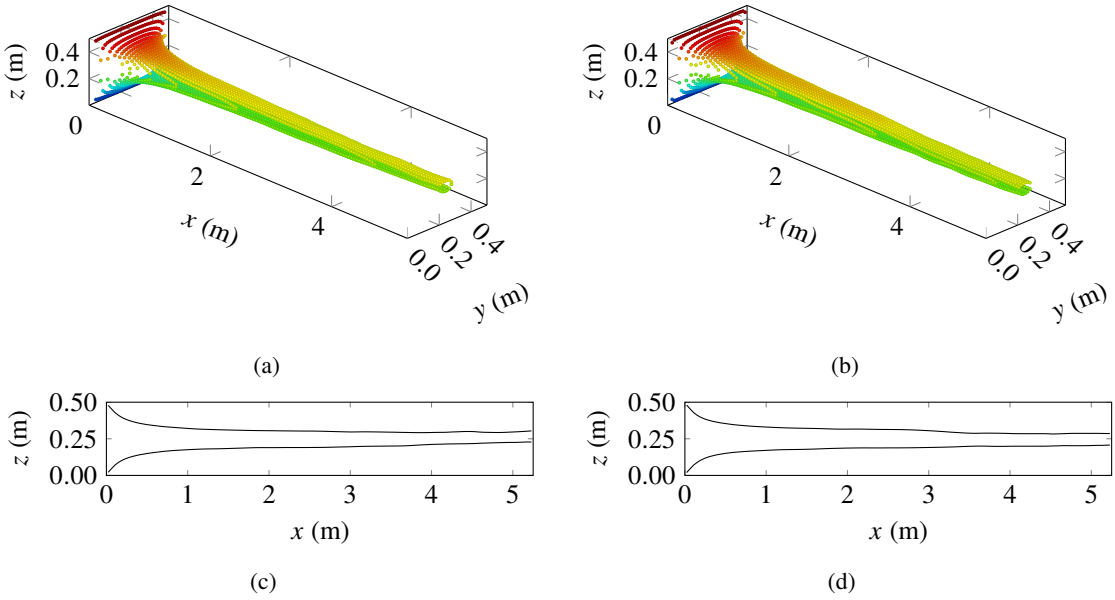

Figure 5: Outlines of the thermal boundary layer for cases with turbulence intensity of the flow at the inlet equal to 10 % and participating medium composed of carbon dioxide (left) and water vapor (right). Top: three-dimensional profiles; bottom: two-dimensional profiles along the central xz plane of the domain.

However, two observations should be made before concluding. First, the exclusion of data pertaining to the inside of the thermal boundary layer is a limited methodology, which was initially proposed as an approach to eliminate or reduce the spikes in relative difference that were observed in the simulations of the cases in study. The validity of such methodology as a way to better represent the global effects of TRI (as opposed to more traditional procedures that include data from the entire domain and use normalized differences for the analysis) was not tested in this paper; this is a more complex subject of investigation, since it requires the evaluation of the importance of the boundary layer for the overall radiative heat transfer problem. Second, it should be noted that the methodology described in this section is applicable only for analyses based on local quantities, such as the radiative heat source; for evaluations of TRI effects based on the mean radiative heat flux at the domain wall or the radiative heat transfer rate, for example (i.e., quantities evaluated at the domain boundaries or integrated along entire surfaces), this methodology is not useful. On the other hand, it is interesting to speculate that, for analyses based on other local quantities such as the mean temperature of a flame, the methodology may provide suitable results for comparisons with experimental data or other numerical studies.

5. CONCLUSIONS

This study presented an analysis on the behavior of the relative difference ψ between the mean volumetric radiative heat source computed considering and neglecting the effects of turbulence-radiation interaction, and was a continuation of a series of studies on TRI on non-reactive flows. In previous studies, the authors had verified abrupt increases, or spikes, in the spatial distribution of ψ, that were not properly explained. Through the observation of two- and one- dimensional profiles of the relative difference along selected planes and lines of the domain, in this paper it was possible to determine that the occurrence of these spikes was due to an increase of the mean radiative heat source from a negative to a positive value inside a small region (or, equivalently, a decrease of this quantity from a positive to a negative value) allied with a relatively poor local spatial discretization.

In the second part of the study, a methodology to address the occurrence of the spikes of ψ was proposed. Firstly, the thermal boundary layer thickness for each simulated case was determined, from which it was verified that the flow does not reach a thermally developed inside the domain. Afterwards, data from grid cells located inside the thermal boundary layer was excluded and the relative difference was recomputed, considering only the core region of the flow. With this approach, the spikes of ψ were completely eliminated, and the resulting field and the statistics derived from it showed a good agreement with previous works on turbulence-radiation interaction on non-reactive problems.

6. ACKNOWLEDGMENTS

This work was supported by a doctoral scholarship by CNPq.

7. REFERENCES

Bergman, T.L., Lavine, T.L., Incropera, F.P. and Dewitt, D.P., 2011. *Fundamentals of Heat and Mass Transfer*, John Wiley & Sons, 7th edition, United States of America.

Cassol, F., Brittes, R., França, F.H.R. and Ezekoye, O.A., 2014. "Application of the weighted-sum-of-gray-gases model for media composed of arbitrary concentrations of H_2O, CO_2 and soot". *International Journal of Heat and Mass Transfer*, Vol. 79, pp. 796–806.

Coantic, M. and Simonin, O., 1984. "Radiative effects on turbulent temperature spectra and budgets in the planetary boundary layer". *Journal of the Atmospheric Sciences*, Vol. 41, n. 17, pp. 2629–2651.

Coelho, P.J., 2007. "Numerical simulation of the interaction between turbulence and radiation in reactive flows". *Progress in Energy and Combustion Science*. Vol. 33, pp. 311–383.

Curry, J.A., 1985. "Interactions among turbulence, radiation and microphysics in Arctic stratus clouds". *Journal of the Atmospheric Sciences*, Vol. 43, n. 1, pp. 90–106.

Dorigon, L.J., Duciak, G., Brittes, R., Cassol, F., Galarça, M. and França, F.H.R., 2013. "WSGG correlations based on HITEMP2010 for computation of thermal radiation in non-isothermal, non-homogeneous H_2O/CO_2 mixtures". *International Journal of Heat and Mass Transfer*, Vol. 64, pp. 863–873.

Duan, L., Martín, M.P., Sohn, I., Levin, D.A. and Modest, M.F., 2011."Study of emission turbulence-radiation interaction in hypersonic boundary layers", *AIAA Journal*, Vol. 49, n. 2, pp. 340–348.

Fraga, G.C., Petry, A.P. and França, F.H.R., 2015. "Influence of the radiative properties of a participating medium on the turbulence-radiation interaction in a non-reacting channel flow". In *Proceedings of the 23rd ABCM International Congress of Mechanical Engineering – COBEM 2015*. Rio de Janeiro, Brazil.

Fraga, G.C., Petry, A.P. and França, F.H.R., 2016. "Analysis of the influence of the spectral dependence of radiative properties of a participating medium in the turbulence-radiative interaction in a non-reacting channel flow". In *Proceedings of the 16th Brazilian Congress of Thermal Sciences and Engineering – ENCIT 2016*. Vitória, Brazil.

Fraga, G.C., Centeno, F.R., Petry, A.P. and França, F.H.R., 2017. "Evaluation and optimization-based modification of a model for the mean radiative emission in a turbulent non-reactive flow". *International Journal of Heat and Mass Transfer*, Vol. 114, pp. 664–674.

Germano, M., Piomelli, U., Moin P. and Cabot W.H., 1991. "A dynamic subgrid-scale eddy viscosity model". *Physics of Fluids A*, Vol. 64, n. 7, pp. 1760–1765.

Gupta, A., Haworth, D.C. and Modest, M.F. "Large-eddy simulation of turbulence-radiation interactions in a turbulent planar channel flow". *Journal of Heat Transfer*, Vol. 131, n. 6.

Howell, J.R., Siegel, R., and Mengüç, M.P., 2010. *Thermal Radiation Heat Transfer*. CRC Press, 5th edition, United States of America.

Jarrin, N., 2008. *Synthetic inflow boundary conditions for the numerical simulation of turbulence*. Ph.D. thesis, University of Manchester, Manchester, United Kingdom.

Lilly, D.K., 1992. "A proposed modification of the Germano subgrid-scale closure method". *Physics of Fluids A*, Vol. 4, n. 3, pp. 633–635.

Mazumder, S. and Modest, M.F., 1999. "Turbulence-radiation interaction in nonreactive flow of combustion gases". *Journal of Heat Transfer*, Vol. 121, n. 3, pp. 726–729.

McGrattan, K., Hostikka, S., McDermott, R., Floyd, J., Weinschenk, C. and Overholt, K., 2017a. *Fire Dynamics Simulator Technical Reference Guide Volume 1: Mathematical Model*. NIST Special Publication, 1018-1, 6th edition, Baltimore, Maryland.

McGrattan, K., Hostikka, S., McDermott, R., Floyd, J., Weinschenk, C. and Overholt, K., 2017b. *Fire Dynamics Simulator User's Guide*. NIST Special Publication, 1019, 6th edition, Baltimore, Maryland.

Modest, M.F., 2013. *Radiative Heat Transfer*. Academic Press, 3rd edition, United States of America.

Prinn, R.G., 1977. "On the radiant damping of atmospheric waves". *Journal of the Atmospheric Sciences*, Vol. 34, pp. 1386–1401.

Raithby, G.D. and Chui, E.H., 1990. "A finite-volume method for predicting radiant heat transfer in enclosures with participating media". *Journal of Heat Transfer*, Vol. 112, n. 2, pp. 415–423.

Rehm, R.G. and Baum, H.R., 1978. "The equations of motion for thermally driven, buoyant flows". *Journal of Research of the National Bureau of Standards*. Vol. 83, n. 3, pp. 297–308.

Santos, E.D., Isoldi, L.A., Petry, A.P. and França, F.H.R., 2014. "A numerical study of combined convective and radiative heat transfer in non-reactive turbulent channel flows with several optical thicknesses: a comparison between LES and RANS". *Journal of the Brazilian Society of Mechanical Sciences and Engineering*, Vol. 36, n. 1, pp. 207–219.

8. RESPONSIBILITY NOTICE

The authors are the only responsible for the printed material included in this paper.